

## An Investigation of The Up and Down End Milling Force Process under Runout and Tilting Effects

Dr. Raed R. Shwaish\* Dr. Muawafak A. Tawfik\*\*  
& Dr. Mohammed J.AL Tornachy\*\*

Received on: 2/ 11 / 2008

Accepted on: 16/2/2010

### Abstract

This paper provides a comprehensive study into cutting forces for (Up and Down) milling process methods either through machine cutting tool errors (Run out and/or Tilting) or not according to vectorial multi-axis rigid cutting force model where flat end mill cutter with peripheral cutting is used. This paper instates a contribution to illustrate the nonsmooth characteristic of milling operation.

Theoretical analysis of the milling process is conducted in this study by simulating the mathematical model of the process through a computer program prepared in FORTRAN language.

The theoretical analysis consists of empirical parameters which are estimated according to measured force data for material cutter and range of cutting conditions taken from references concerned with numerical simulation of milling process.

**Keywords:** Milling Forces, Flute engagement, Simulated cutting forces.

### بحث لعملية قوة تفريز طرفي صاعد ونازل تحت تأثيرات الخروج والأماله

#### الخلاصة

يُزوّد هذا البحث دراسة شاملة لقوى القطع لطرق عملية التفريز (الصاعد والنازل) أما بوجود أخطاء أداة قطع الماكينة (الخروج و/ أو الأماله) او عدم وجودها، طبقاً لنموذج قوة قطع جاسئ إجهائي متعدّد المحور حيث إستعمل قاطع طرفي مستوي النهاية في عملية قطع خارجية. هذا البحث يضع مساهمة لتصوير السمة غير السهلة لعملية التفريز. تحليل نظري لعملية التفريز مجرى في هذه الدراسة يتمثل النموذج الرياضي من العملية خلال برنامج حاسوب معدّ بلغة الفورتران. التحليل النظري يتضمّن البارامترات التجريبية المُخمنّة طبقاً لبيانات القوة المقاسة لمادة القاطع ومدى ظروف قطع أخذاً من مصادر مُهتمة بالمحاكاة العددية لعملية التفريز.

### 1. Introduction

Milling is a multiple point, interrupted cutting operation. Because of the multiple teeth, the engagement time of each individual tooth is a fraction of the total time of one single

tool rotation. The finished surface, accordingly, consists of a series of elemental surfaces generated by the individual cutting edges of the cutter, [1-1994s]. Due to the general motion of the cutter relative to the workpiece, the uncut (undeformed) chip

\*Production and Metallurgy Engineering Department, University of Technology/ Baghdad

\*\* Machines & Equipments Engineering Department, University of Technology/ Baghdad

thickness is not constant but, for down milling it starts with a finite thickness and decreases to zero while for up milling it starts with zero thickness and increases to finite thickness, as illustrate in Fig. (1).

The very early research in milling mechanics dealt with the chip formation mechanism and spindle power estimation. Martelloti's work on the geometry of the milling process established the definition of the tool path and instantaneous chip thickness [2-1941s] & [3-1945s]. Martelloti showed that the true path of a milling cutter tooth is trochoidal, but it can be approximated as circular if the radius of the cutter is much larger than the feed per tooth, see Fig. (2).

For this case the chip thickness is given by:

$$t_c = S \cdot \sin(\beta) \quad \dots\dots\dots(1)$$

Where, S and  $\beta$  are the feed per tooth and tooth engagement angle respectively.

The term mechanistic force model, which was adopted by many researchers in the analysis of the milling process, is usually referred to as an approach for the milling force calculation in which the cutting force is related to the undeformed chip thickness through coefficients based on the assumptions [4-1980s]:

1- The tangential cutting force is proportional to the chip load,

$$F_t = K_t \cdot C_L \quad \dots\dots\dots(2)$$

2- The radial cutting force is proportional to the tangential cutting force,

$$F_r = K_p \cdot C_L = (K_r \cdot K_t) \cdot C_L \\ = K_r \cdot F_t \quad \dots\dots\dots(3)$$

where (Kt & KP & Kr) are empirical cutting constants; Kt is the specific

cutting pressure or tangential cutting pressure constant, KP is the thrust or radial pressure constant, Kr is ratio of radial to tangential cutting force; CL instantaneous chip load, which represents the multiplication of axial depth of cut Ad by instantaneous chip thickness tc, i.e.

$$C_L = t_c \cdot A_d \quad \dots\dots\dots(4)$$

In general, cutting force models developed for the milling process consist of the following two fundamental assumptions:

1- The kinematics of milling can be modeled by decoupling the motions of spindle and table. As a result, the cutting edge path can be assumed circular, and equation (1) can be used for the chip thickness.

2- The mechanics of machining of any complex process can be modeled by an aggregation of oblique cuts, if the cutting edge is divided into infinitesimal elements. The application of this assumption is to discretize the tool into thin slices, calculate the cutting force applied to each slice of the discretized tool using equations (2) & (3) and then sum up the differential cutting forces for all the slices and teeth engaged along each coordinate direction. To gain higher speed in calculation of cutting forces some researchers have explicitly integrated the expressions of cutting force for flat end mills [5-1989s] & [6-1991s].

**2- Model Work**

**2-1- Rigid Cutting Force Model**

The model studied here is used for rigid down and up end milling with right hand helix cutting tool and the basic modeling depends on describing the cutting tool according to its Geometrical Variables [7-2000s]:

1- Cutting tool with teeth noted by (K), where ( $N_f$ ) is the total number of teeth. The space angle between each successive two teeth (i.e. cutter pitch angle) noted by ( $\gamma$ ), is calculated by:

$$g = \frac{(2.0) \cdot p}{N_f} \dots\dots\dots(5)$$

2- Cutting tool with slides elements as discs is noted by (I) just along the axial engagement part of the cutting tool with the workpiece, i.e. Axial Depth of Cut ( $A_d$ ). ( $N_z$ ) is the total number of the slides, these axial slides are equal in axial thickness ( $D_z$ ) where:

$$D_z = \frac{A_d}{N_z} \dots\dots\dots(6)$$

To specify the center height [Z(I)] of each slide with respect to the free end of the cutting tool; the following is adopted:

$$Z(I) = (I-1.0) \cdot D_z + \frac{D_z}{(2.0)} \dots\dots(7)$$

3- Angular increment of cutting tool rotation is noted by (J), where ( $N_q$ ) is the total angular increments, which equal one revolution ( $360^\circ$ ) taken with respect to the free end of the cutting tool at the arbitrary first chosen tooth. So the instantaneous angular position [ $q(J)$ ] is according to:

$$q(J) = (2.0) \cdot p \cdot \frac{J}{N_q} \dots\dots\dots(8)$$

The helix angle ( $\alpha_h$ ) causes change in the magnitude of Engagement Angle ( $b$ ) at the center of each slide from its side in the direction of the free end of the cutting tool. The

change in the angle is calculated from the resiling angle ( $a_d$ ), which represents angle measured back as the engagement progresses up the helix.

The resiling angle ( $a_d$ ) is calculated according to:

$$a_d(I) = Z(I) \cdot \frac{\tan(\alpha_h)}{Rad_o} \dots\dots\dots(9)$$

Therefore, engagement angle ( $b$ ) according to the influence of magnitude of (K & I & J) with respect to the free end yields:

$$b(J, I, K) = -q(J) + g(K-1.0) + a_d(I) \dots\dots\dots(10)$$

So the instantaneous chip thickness is calculated according to:

$$t_c(J, I, K) = S \cdot \sin b(J, I, K) \dots\dots(11)$$

And instantaneous chip load is calculated according to:

$$Cl(J, I, K) = D_z \cdot t_c(J, I, K) \dots\dots(12)$$

And the instantaneous tangential and radial cutting forces are calculated according to:

$$dF_t(J, I, K) = K_t \cdot C_L(J, I, K) \dots\dots(13)$$

$$dF_r(J, I, K) = K_r \cdot dF_t(J, I, K) \dots\dots(14)$$

The forces above are introduced in the rotation coordinates (tangential & rotational). So transfer matrix [D] is used to introduce them in the Cartesian coordinates, which is dependent on the feeding method

$$\left. \begin{aligned} [D(J, I, K)]_{down} &= \begin{bmatrix} -\sin b & \cos b \\ \cos b & \sin b \end{bmatrix} \\ [D(J, I, K)]_{up} &= \begin{bmatrix} -\sin b & -\cos b \\ \cos b & -\sin b \end{bmatrix} \end{aligned} \right\} \dots\dots(15)$$

Where the center of Cartesian coordinates at the origin in the center of the cutter, the X-axis is in the opposite direction of the feed, the Z-axis is normal to the workpiece surface up in the direction of the

cutter axis and Y-axis is found from the right hand rule. See Fig. (3).

Therefore, the forces obey to:

$$\begin{Bmatrix} dF_x(J,I,K) \\ dF_y(J,I,K) \end{Bmatrix} = [D(J,I,K)].$$

$$\begin{Bmatrix} dF_r(J,I,K) \\ dF_t(J,I,K) \end{Bmatrix} \dots(16)$$

The formula above use to calculate the forces applied on one tooth only. Since there are number of teeth, therefore, there are chance to be more than one tooth in engagement with the workpiece at same time. Therefore, the forces applied on any slides of the tool at any moment (any rotation angle of the tool) are the sum of all force components applied on each tooth in the engagement with the workpiece, see Fig. (4). and then the formula became:

$$\begin{Bmatrix} DF_x(J,I) \\ DF_y(J,I) \end{Bmatrix} = \sum_{K=1}^{N_t} d(J,I,K) \cdot [D(J,I,K)].$$

$$\begin{Bmatrix} dF_r(J,I,K) \\ dF_t(J,I,K) \end{Bmatrix} \dots\dots(17)$$

Where  $d(J,I,K)$  is tooth engagement factor so:

$$d(J,I,K) = \begin{cases} 1.0 & \text{if } a_{ext} \leq b(J,I,K) \leq a_{int} \\ 0.0 & \text{otherwise} \end{cases} \dots(18)$$

To estimate the total forces act on all slides of the tool in direction (X & Y) at specified position then:

$$\begin{Bmatrix} F_x(J) \\ F_y(J) \end{Bmatrix} = \sum_{I=1.0}^{N_s} \begin{Bmatrix} DF_x(J,I) \\ DF_y(J,I) \end{Bmatrix} \dots\dots\dots(19)$$

The average forces predicted in directions (X & Y) for all the angular positions become:

$$\begin{Bmatrix} F_{xp} \\ F_{yp} \end{Bmatrix} = \frac{(1.0)}{N_q} \cdot \sum_{J=1.0}^{N_h} \begin{Bmatrix} F_x(J) \\ F_y(J) \end{Bmatrix} \dots\dots\dots(20)$$

**2-2- Nonlinearities Cutting Force Dynamics:-**

Often all force models adopt linear force model while cutting process includes essentially nonlinearities such as machine cutting tool errors (Run out & Tilting) which are produced from defect between tool holder mechanism and machine spindle, these errors are not easy to be measured and affect the cutting processes [8-1996s].

**2-2-1- Run out**

In the previous rigid cutting force model there are no machine cutting tool errors, the three direction representations of milling tool display that the cutting forces estimation depends on instantaneous chip thickness  $(t_c(J,I,K))$  calculated from Eq. (11). But if there are run out effect, then this equation should be modified to include the changeable radius of milling cutting teeth with respect to the rotating axis, where the offset teeth toward holder rotating axis have effective radius greater than the teeth on the opposite side of the milling cutting tool. For the helix tool ( $a_h \neq 0.0$ ), the run out does not conjugate with specific tooth but with specific side named by the height side of the tool. While for tool with ( $a_h = 0.0$ ), the run out conjugates with specific tooth. The run out could be divided to [9-1983s]:

- 1- Radial Run out ( $R_n$ ) which represents the axial offset of the tool axis with respect to the rotating axis. Its magnitude is constant along tool axis when there is no tilting effect.
- 2- Angular Run out ( $a_{Rn}$ ) which represents the angle measured at the free end of the tool between the radial run out direction and the nearest tooth

to the radial run out direction. This tooth will be considered the first tooth to enter the engagement, see Fig. (5).

Estimation of the effective radius for specific tooth with specific magnitude for radial run out and angular run out is also dependent on feeding method; therefore the formulas used are [7-2000s]:

$$\begin{aligned}
 Rad(I, K)_{down} &= \left\{ \begin{aligned} &Rn^{2.0} + (2.0).Rn.Rad_o. \\ &\cos[a_d(I) + g(K-1.0) - a_{rn}] \\ &+ Rad_o^{2.0} \end{aligned} \right\}^{0.5} \\
 Rad(I, K)_{up} &= \left\{ \begin{aligned} &Rn^{2.0} + (2.0).Rn.Rad_o. \\ &\cos[a_d(I) - g(K-1.0) - a_{rn}] \\ &+ Rad_o^{2.0} \end{aligned} \right\}^{0.5} \quad \dots(21)
 \end{aligned}$$

Which declare that any tooth radius does not depend on the rotation angle of the tool. Then the formula can be derived for estimation of the instantaneous chip thickness including tool run out as difference between radius of the engagement tooth and the previous one as given below:

$$DRad(I, K) = Rad(I, K) - Rad(I, K - 1.0) \quad \dots(22)$$

$$t_c(J, I, K) = S \cdot \sin b(J, I, K) + DRad(I, K) \quad \dots(23)$$

The above equations are derived when the radial run out ( $Rn$ ) is small compared with the feed( $S$ ), either the high side of the tool only does cut, the change in radius from tooth to another produce by run out might be negative and greater than  $S \cdot \sin b$ , therefore there is no cutting .but really the tooth cutting the workpiece leaves tooth or more pass without cutting that part.

The modeling of run out affects the force system for any run out by considering chosen tooth ( $K$ ), chosen disc ( $I$ ) and satisfying  $d(J, I, K) = 1.0$ , then correcting

instantaneous chip thickness for all teeth at that element (disc), and finding the tooth that has greater radius, next estimate the instantaneous chip thickness for the following tooth according to the formula below :

$$t_c(I, J, K) = S \cdot \sin b(I, J, K) + DRad(I, K) + M(K) \quad \dots(24)$$

Fixing magnitude  $M(K) = 0.0$  at that tooth, if chip thickness is negative, equal to zero but its magnitude is preserved for next tooth in ( $M(K + 1.0) = 0.0$ ), and it is repeated for all teeth. After correcting instantaneous chip thickness for all teeth of that element take the instantaneous chip thickness for specific tooth first which originally specified its ( $J$  &  $I$  &  $K$ ) in  $d(J, I, K)$ . As  $M(K)$  is a negative constant also if ( $K = 1.0$ ) then:

$$Rad(I, K - 1.0) = Rad(I, N_f) \quad \dots(25)$$

### 2-2-2- Tilting

If Tilting effect exists then the instantaneous chip thickness is calculated from equation (11) also its effect is like run out effect. Therefore, you must correct the instantaneous chip thickness to include changing effect in radius of milling cutting tool conjugated along axial depth of cut with respect to rotating axis.

Therefore, the tilting teeth toward the holder at the free end has effective radius greater than the teeth on the opposite side of the tool and also greater effective radius than the teeth on the same side of the tool but at the elements are far away from the free end of the tool.

Tilting is defined by [10-1986s]:

1- Axial Tilting ( $Ti$ ); which represents tilting angle of the tool axis with respect to the rotating angle.

2- Angular Tilting ( $a_{Ti}$ ); which represents angle like angle of angular run out where it is measured from the free end of the tool between the axial tilting direction and the nearest tooth to the axial tilting direction. This tooth will be considered as the first tooth to enter the engagement, see Fig. (6).

Estimation of the effective radius for specific tooth at specific element with specific magnitude for axial tilting and angular tilting is according to the following formula [7-2000s]:

$$\left. \begin{aligned}
 Rad(I, K)_{down} &= \left\{ \begin{aligned}
 &[(L - Z(I)) \cdot \sin(Ti)]^{2.0} + \\
 &(2.0) \cdot (L - Z(I)) \cdot \sin(Ti) \cdot Rad_o \cdot \\
 &Cos[a_d(I) + g(K - 1.0) + a_{Ti}] \\
 &+ Rad_o^{2.0}
 \end{aligned} \right\}^{0.5} \\
 Rad(I, K)_{up} &= \left\{ \begin{aligned}
 &[(L - Z(I)) \cdot \sin(Ti)]^{2.0} + \\
 &(2.0) \cdot (L - Z(I)) \cdot \sin(Ti) \cdot Rad_o \cdot \\
 &Cos[a_d(I) - g(K - 1.0) + a_{Ti}] \\
 &+ Rad_o^{2.0}
 \end{aligned} \right\}^{0.5}
 \end{aligned} \right\} \dots(26)$$

Here instantaneous chip thickness will be corrected in the same way as that used in run out effect case.

### 2-3- Identification of Cutting Parameters [Specific Cutting Pressure (Kt) and Tool Geometric Constant (Kr)]:-

The parameters Kt and Kr are obtained from a database of machining conditions and then empirical models are developed from these data to predict Kt and Kr for any set of machining conditions within the data base. Numerous investigators have directed attention toward the determination of specific cutting pressure, Kt, and developed a number of different models. Since Kt and Kr are to be modeled as function of chip thickness tc, they really will be functions of almost all cutting conditions.

In milling processes, the chip thickness continuously changes along the tooth path.

However, using an instantaneously changing  $Kt(\theta)$  for evaluating instantaneously forces is not practical. Martellotti [2-1941s] & [3-1945s] and Koenigsberger and sabberwal [11-1960s] & [12-1961s] found that average chip thickness also has a definite relationship.

An approach has been used where the parameters of the force model, Kt and Kr, may be estimated from measured average X and Y forces. For a particular cut geometry (axial depth, radial depth and feed rate), the values for Kt and Kr may be obtained by expressing the average forces Fxp and Fyp in terms of X and Y forces and then summing over the angular position  $\theta(J)$  for  $J=1,2,\dots,N\theta$  where  $N\theta$  is the number of angular increments as given in Eq. (20).

Both  $F_x(J)$  and  $F_y(J)$  can be expressed solely as function of Kt, Kr, S, Dz and  $\beta$  from equations (5→20). Therefore, average X and Y forces (for down milling, as example) are given by:

$$F_{xp} = \frac{1}{N_q} \cdot \sum_{J=1}^{N_q} \sum_{I=1}^{N_I} \sum_{K=1}^{N_K} \left\{ \begin{aligned}
 &K_r K_t D_z S \cdot \\
 &Sin[b(I, J, K)] \cdot \\
 &Cos[b(I, J, K)] \\
 &+ K_t D_z S \cdot \\
 &Sin^2[b(I, J, K)]
 \end{aligned} \right\} \dots(27)$$

$$F_{yp} = \frac{1}{N_q} \cdot \sum_{J=1}^{N_q} \sum_{I=1}^{N_I} \sum_{K=1}^{N_K} \left\{ \begin{aligned}
 &K_r K_t D_z S \cdot \\
 &Sin^2[b(I, J, K)] \\
 &+ K_t D_z S \cdot \\
 &Sin[b(I, J, K)] \cdot \\
 &Cos[b(I, J, K)]
 \end{aligned} \right\} \dots(28)$$

For  $a_{exit} \leq b(J, I, K) \leq a_{ent}$ .

Having found the average measured forces Fxp and Fyp, equations (27 & 28) may be solved for Kt & Kr for each cutting condition. Regression

analysis by the Least Squares Method which has been applied to  $K_t$ ,  $K_r$  and  $T$ , for the average chip load. The resulting mathematical equations are as follows:

$$\left. \begin{aligned} K_t &= I_t \cdot (T)^{-I_a} \\ K_r &= I_r \cdot (T)^{-I_b} \end{aligned} \right\} \dots(29)$$

where  $I_t$ ,  $I_a$ ,  $I_r$  and  $I_b$  are positive constants.

The entire mechanistic force modeling procedure is represented graphically in Fig. (7). The spirit of this approach is, given empirical data on average forces from statically designed experiments for rectangular cut cross-sections, the mechanistic force model can be employed to study the force system in more detail. The model may be used to study instantaneous force distributions, cutter deflection characteristics, the effects of the force system on cutter breakage and/or surface roughness and surface accuracy considerations.

### 3- Results & Discussions:-

#### 3-1- Verification of Cutting Parameters and Force Model:-

The model building approach has been verified through the comparison of:-

1- The predicted parameters  $K_t$  and  $K_r$ , Table (1).

2- Measured and predicted average and instantaneous forces, Table (2).

Which are obtained from the Machining Data base for (7075-T6 Aluminum) workpiece[9-1983s]. The experiments were performed with four flute high speed steel end mills, Helix (30 deg.), Flute length (44.45 mm), diameter (19.05 mm). Instantaneous X and Y force signals were measured and recorded using a strain ring platform dynamometer and

a microprocessor controlled data acquisition system. The sampling rate was(680 samples/sec). A set screw-type tool holder was used. The run out offset was measured to be (0.0254 mm) for the end mill used in the tests, the locating angle was measured to be (15 deg.). Cutting speed (509.295 rev/min). Cutter tilt was negligible and no coolant was used.

The percentage differences between measured and predicted average forces range from (5→10%) indicating that the model building approach and  $K_t$  and  $K_r$  models provide a reasonably accurate method for the prediction of average forces [14-1982s].

#### 3-2- Geometrical Modeling Variables:-

The geometrical modeling of the cutter is characterized by the variables  $N\theta$ ,  $Nz$ ,  $Nf$ ,  $L$ ,  $ah$  and  $Rado$ . In this study case  $N\theta=360$ , and  $Nz=10$  are adopted to get good demonstration of the model and it is enough to have precision. Since it is considered as a rigid force model then there is no flexibility for the tool and does not affect the machining forces.  $L=72\text{mm}$  is fixed. The entry angle ( $\alpha_{ent}$ ) for down milling or exit angle ( $\alpha_{exit}$ ) for up milling is considered (78.46o) which is calculated from [2-1941s]:-

$$\begin{aligned} \alpha_{ent-down} &= \alpha_{exit-up} \\ &= \text{Cos}^{-1} \left[ 1 - \frac{R_d}{Rad_o} \right] \end{aligned} \dots(30)$$

In figures (8→14), the sections a&b shows cutting forces for each slice with angular location for Y&X directions respectively, While sections c shows cutting forces in (X&Y) directions for the cutting tool (all axial slices  $Nz$ ) with angular location.

**3-2-1- Cutter Geometrical Variables****\*\* Two-Tooth Straightforward End Mill:**

According to equation (5), cutter pitch angle ( $\beta$ ) is  $(180^\circ)$ . And according to straightforward, the engagement of any tooth is at the same time for all slices of the cutting tool along its axial depth of cut, Fig. (8- 1&2).

**\*Down milling;**

Cutting force acts always in the positive Y direction, therefore the force reaction acting on the workpiece gives hard mounting for workpiece. While cutting force in the X-direction (feed direction) is less in magnitude than its value in Y-direction, and it is reversed in direction sign. It can be in positive or negative direction only or at first in negative direction, which reverses to positive direction, according to radial depth of cut Rd. If this reversion coincides in direction with sudden vibration, this may allow the tool to climb the workpiece causing tool breakage. For that reason, down milling is called climbing milling, Fig. (8- c-1).

**\*Up milling;** Cutting force acts in the Y-direction reversed in direction sign. It can be in positive or negative direction only or at first in positive direction, which reverses to negative direction, according to radial depth of cut Rd. This reversion will influence surface finish of the workpiece. While cutting force in the X-direction (feed direction) is less in magnitude than its value in Y-direction but greater than that in down milling, and it acts always in the negative X-direction, therefore its reaction on the workpiece tries to lift the workpiece, and thus named Up milling. So this

milling needs enough fixing of the workpiece to withstand the reaction, Fig. (8- c-2).

**\*\* Four-Tooth Straightforward End Mill**

According to equation (5), cutter pitch angle ( $\gamma$ ) is  $(90^\circ)$ . Here we see same cutting performance for 2-tooth straightforward end mill but with reducing cutting absence period, since the calculated cutting forces depend on the instantaneous chip thickness, which is calculated from the feed per tooth. Fig. (8- 3&4).

**3-2-2- Helix Angle Effect**

Increasing teeth number leads to have continuous cutting process depending on design finite possibilities, which are concerned with end mill diameter. Therefore, helix comes as the possible solution besides it helps to take away the chip from the cutting region. Helix changes sequence of enter engagement for tooth slices along end mill axis because of the resiling angle ( $\alpha_d$ ) calculated from Eq. (9) which affects Engagement Angle ( $\beta$ ) according to Eq. (10). This makes slices seriatim enter and exit the engagement hence, reducing cutting absence period and cutting force peak.

**\*\* Two-Tooth Right Helix End Mill:**

**\*Down milling;** Here cutting starts with tooth number one, instead of two in straightforward end mill, but with the above slices, element one ( $I=1$ ) doesn't cut. However, the other slices are under cut in different amount of chip thickness according to the angular location and the Engagement Angle ( $\beta(J, I, K)$ ), so different cutting forces are generated. These slices of tooth number one exit sequentially from the engagement, as the cutter rotates. Then a period of cutting

absence engagement occurs before cutting begins again with enter tooth number two at the slice number one ( $I=1$ ), i.e. at the free end of the end mill after the tool rotates ( $101.537^\circ$ ) which is considered as a complement angle to the entry angle. Then the process is repeated, Fig. (9- a&b 1).

**\*Up milling;** As tool starts rotating, cutting process begins with tooth number one in different amount of chip thickness according to the angular location and the Engagement Angle ( $\beta(J, I, K)$ ), so different cutting forces are also generated. These slices of tooth number one leave the engagement sequentially after the tool rotates ( $78.46^\circ$ ) which is the exit angle. Then a period of cutting absence engagement occurs before cutting begins again with enter tooth number two at the slice number ten ( $I=10$ ). Then the process is repeated, Fig. (9- a&b 2).

**\*\* Four-Tooth Right Helix End Mill:** Under the same conditions applied in the above cited, Fig. (9- 3&4) shows hidden cutting absence period to have continuous swinging cutting. Now it is difficult to recognize cutting tooth region because of the overlapping of the engaged teeth with the workpiece.

### 3-3- Run Out Effect

**\*\* Two-Tooth Straightforward End Mill:**

For straightforward end mill, run out conjugates with specific tooth which suffers from cutting forces more than others, Fig. (10- 1&2).

**\*Down milling;** Fig. (10- a&b&c1), Since entry angle is ( $78.46^\circ$ ) tooth number two enters engagement at the complementary angle ( $101.537^\circ$ ) and since this tooth is displacing from the workpiece therefore this tooth will meet smaller chip thickness consequently smaller cutting forces

also this tooth exit the engagement early compared with run out absence. See Fig. (8- a&b 1). As cutting continues with tooth number one enters engagement at angle ( $281.537^\circ$ ), this tooth will meet bigger chip thickness consequently higher cutting forces but this tooth exits the engagement at angle ( $360^\circ$ ). i.e., the engagement does not exceed the angle ( $78.46^\circ$ ) as in tooth number one but it could be less than ( $78.46^\circ$ ) as in tooth number two.

**\*Up milling;** Fig. (10- a&b&c 1), As cutting starts, tooth number one enters engagement directly and since this tooth is brought near the workpiece, therefore this tooth will meet bigger chip thickness consequently higher cutting forces compared with run out absence case, see Fig. (8- a&b 2). Then this tooth exits engagement at exit angle ( $78.46^\circ$ ). As cutting continues, tooth number two enter engagement behindhand and meets smaller chip thickness consequently smaller cutting forces since this tooth is displacing from the workpiece.

**\*\* Two-Tooth Right Helix End Mill:**

For helix end mill, runout conjugates with the height side of the end mill which suffers from cutting forces more than others.

By comparing Fig. (10) for straightforward end mill with Fig. (11) for helix end mill, one notices a wide spread cutting region is available but with a reduction in the magnitude of the peak cutting force as expected from section (3-2-2). Increasing end mill's number of teeth changes distribution of cutting chip thickness. Fig. (11- 3&4) shows cutting forces behavior for 4-tooth helix end mill when run out exists. It is the most confusing situation since

all the elements along axial depth of cut engage at any location with different chip thickness due to helix and run out effects.

Radial runout effect on ratio of (maximum per average) resultant cutting force. It can be observed that radial runout increasing increases this ratio. In addition as the cutting is interrupted end cutting this ratio is increased, Fig. (12).

### 3-4- Tilting Effect:-

#### \*\* Two-Tooth Straightforward End Mill:

Tilting focuses the forces on end side of the axial depth of cut for specific tooth when straightforward end mill is used more than others end side and teeth, Fig. (13- 1&2).

**\*Down milling;** Fig. (13- a&b&c1), Since entry angle is  $(78.46^\circ)$  tooth number two enter engagement at the complementary angle of  $(101.537^\circ)$  and since this tooth is tilted far away from the workpiece this tooth will meet smaller chip thickness, compared with tilting absence, Fig. (9- a&b 1), and different chip thicknesses as axial elements  $(I=1 \rightarrow 10)$  are far from the free end of the end mill, compared with run out existence, Fig. (10- a&b 1). Therefore, this tooth will suffer different and smaller cutting forces along its axis. In addition, this tooth exits the engagement early. As cutting continues tooth number one enters engagement at angle of  $(281.537^\circ)$ , this tooth will meet different and bigger chip thickness as axial elements  $(I=1 \rightarrow 10)$  close to the free end of the end mill consequently different and higher cutting forces are expected since this tooth is tilted toward the workpiece. This tooth exits the engagement at angle of  $(360^\circ)$ . i.e., the engagement does not

exceed the angle  $(78.46^\circ)$  as in tooth number one but it could be less than  $(78.46^\circ)$  as in tooth number two.

**\*Up milling;** Fig. (13- a&b&c2), As cutting starts, tooth number one enters engagement directly and since this tooth is tilted toward the workpiece, this tooth will meet different and bigger chip thicknesses as axial elements  $(I=1 \rightarrow 10)$  close to the free end of the end mill consequently different and higher cutting forces in comparison with tilting absence are expected, Fig. (8- a&b 2), or run out existence. Fig. (10- a&b 2). Then this tooth exits engagement at exit angle of  $(78.46^\circ)$ . As cutting continues, tooth number two enters engagement behindhand and meets different and smaller chip thicknesses as axial elements  $(I=1 \rightarrow 10)$  far of the free end of the end mill consequently different and smaller cutting forces are expected since this tooth is tilted away from the workpiece.

#### \*\* Two-Tooth Right Helix End Mill:

For helix end mill, Tilting focuses the forces on the end side of the axial depth of cut for the height side of the end mill more than others.

By comparing Fig. (13) for straightforward end mill with Fig. (14) for helix end mill, a wide spread cutting region is available but with a reduction in the magnitude of the peak cutting force as expected from section (3-2-2).

Fig. (15) shows Axial Tilting effect on ratio of (maximum per average) resultant cutting force. It can be noticed that axial tilting increasing increases this ratio and the tool overhang length reducing reduces this ratio. In addition as the cutting interrupts end cutting this ratio is increased.

**4- Conclusions**

- 1- Increasing teeth number to avoid impact problems and continuous cutting is achieved which reduces cutting absence period and increases tooth passing frequency.
- 2- Using helix end mill which reduces cutting absence period and peak cutting force.
- 3- In general, cutting force component in Y-direction (normal to the machined surface) is higher in magnitude than that in X-direction (feed Direction) for down milling method. On the other hand, the reversal case is for up milling method.
- 4- Elimination or reduction of machine cutting tool error parameters reduces appearance chance of interrupted cutting and replaces tooth passing frequency by force signal frequency.
- 5- Runout parameter focuses forces on one side of cutter more than the others while tilting parameter focuses forces on one free end side of cutter more than the others.

**5- References**

- [1]- Sandvik Coromant, "Modern Metal Cutting", Sweden, 1994.
- [2]- Martellotti, M.E., "An Analysis of the Milling process", Trans. ASME, Vol. 63, 1941, P.667.
- [3]- Martellotti, M.E., "An Analysis of the Milling process. Part II: Down Milling", Trans. ASME, Vol. 67, 1945, P.233.
- [4]- R.E. Devor, W.A. Kline & W.J. Zdeblick: "A Mechanistic Model For The Force System in End Milling With Application To Machining Airframe Structures ", Proc. Of The 8th North American Manufacturing Res. Conf., Vol.8, (1980), pp. (297).
- [5]- Jain S. and Yang K. C. H., "A systematic force analysis of the milling operation", Proc. ASME winter annual meeting, San Francisco, 1998, pp. 55-63.
- [6]- Altintas Y. and Spence A. D., "End milling force algorithms for CAD systems. CIRP Annals, 40 (1), 1991, pp. 31-34.
- [7]- Raed R. Shwaish, "Computer Modeling and Simulation of Cutting variables and Machining Errors on Milling process", M.Sc. (Eng.) Thesis, Department of Machines & Equipments Engineering, University of Technology, Baghdad, Iraq, 2000.
- [8]- Robert G. Landers, A. Galip Ulsoy, "Chatter analysis of Machining systems with Nonlinear Force Processes", ASME International Mechanical Engineering Congress and Exposition, Atlanta, Georgia, November 17-22, DSC Vol.58, 1996, pp. 183-190.
- [9]- W.A. Kline & R.E. Devor: "The Effect of Runout on Cutting Geometry and Forces in End Milling", Int. J. Mach. Tool Des. Res., Vol. 23, No.23, (1983), pp. (123-140).
- [10]- J.W. Sutherland & R.E. Devor: "An Improved Method For Cutting Force And Surface Error Prediction in Flexible End Milling Systems", Journal of Engineering For Industry, ASME transaction, Vol.108, (1986), pp. (108-279).
- [11]- F. Koenigsberger & A.J.P. Sabberwal: "Chip Section And Cutting Force During The Milling Operation", Annals of The CIRP, (1960).

- [12]- F. Koenigsberger & A.J.P.Sabberwal: "An Investigation Into The Cutting Force Pulsations During Milling Operations", Int. J. Mach. Tool Des.Res, Vol.1, (1961), pp. (15-23).
- [13]- Raed R. Shwaish, "Static and Dynamic Analysis of Regenerative Chatter in Vertical Milling Machine", Ph.d. (Eng.) Thesis, Department of Production and Metallurgy Engineering, University of Technology, Baghdad, Iraq, 2008.
- [14]- W. A. Kline, R. E. Devor, J. R. Lindberg, the prediction of cutting forces in end milling with application to cornering cuts, Int. J. Mach. Tool Des. Res. Vol. 22, 1982, pp. (7-22).

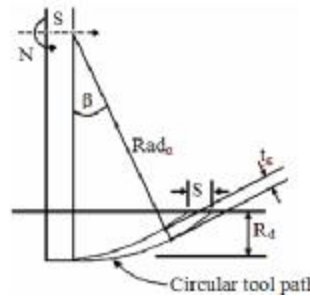


Figure (2) Chip Thickness variation in the peripheral milling.

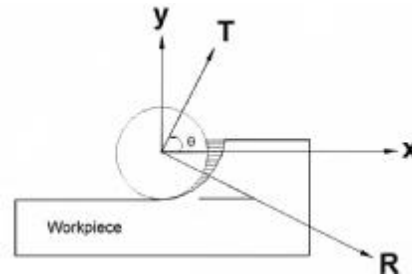


Figure (3) Rotating and Cartesian Coordinates.

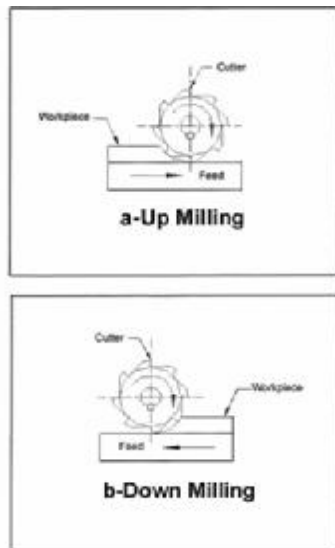


Figure (1) Milling methods.

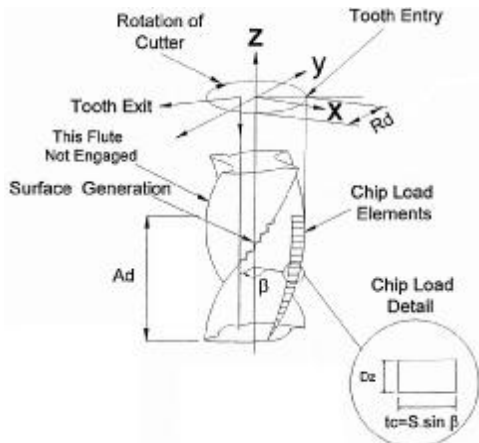


Figure (4) End mill cutting tool modeling.

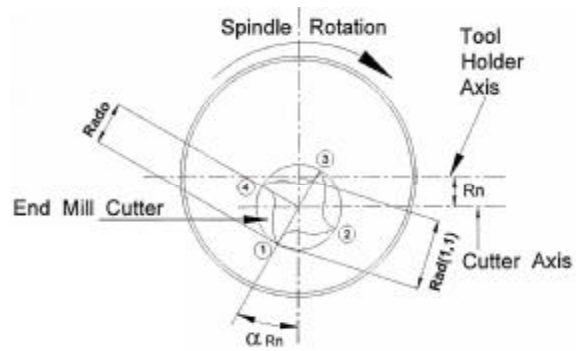
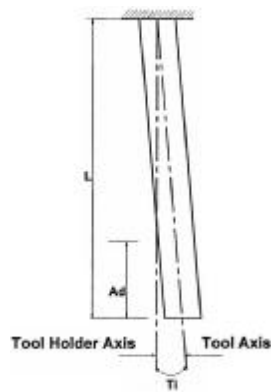
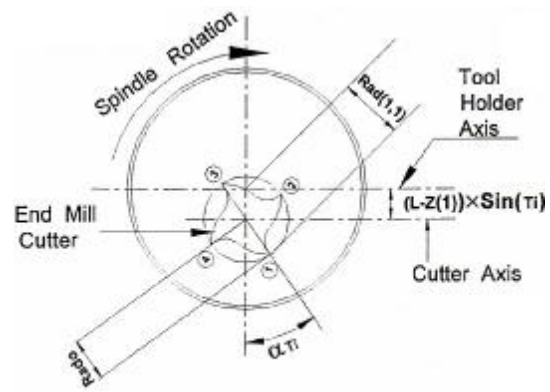


Figure (5) Tool run out demonstration with down milling process.



-a-



-b-

Figure (6) Tool tilting demonstration with down milling process.  
[ a- Side View. b- Top View.]

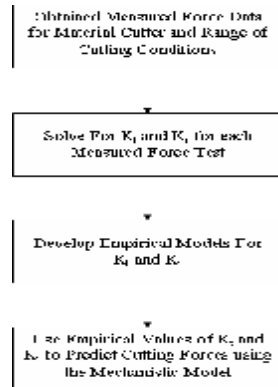


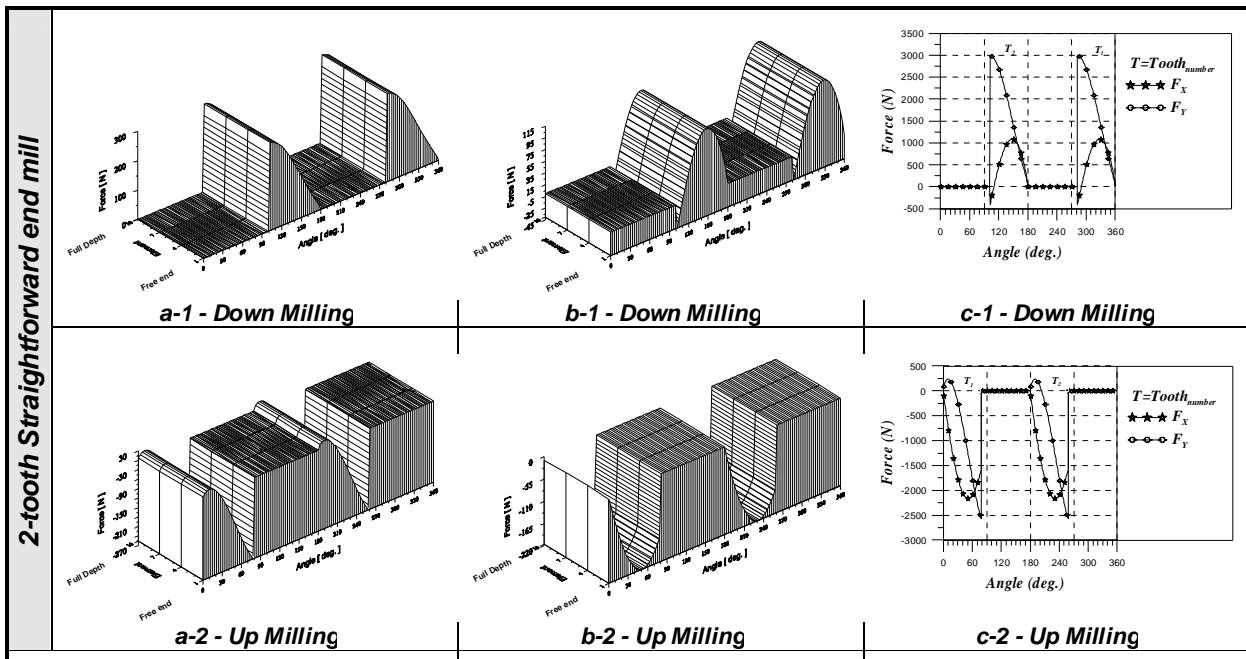
Figure (7) Flowchart of mechanistic modeling procedure

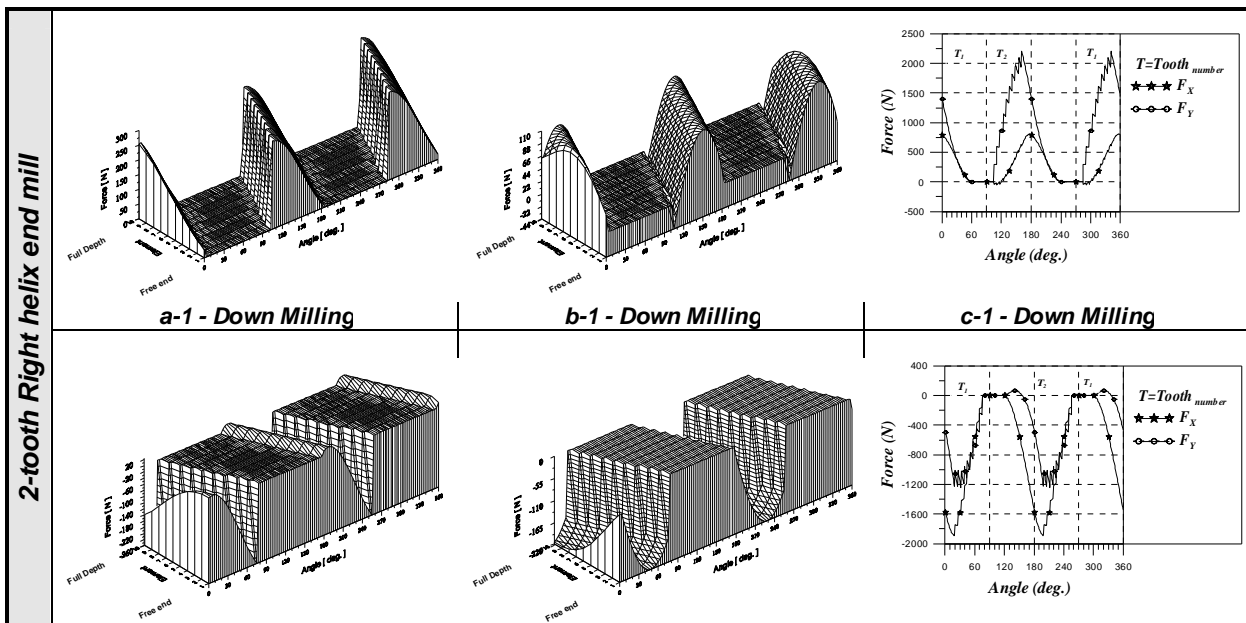
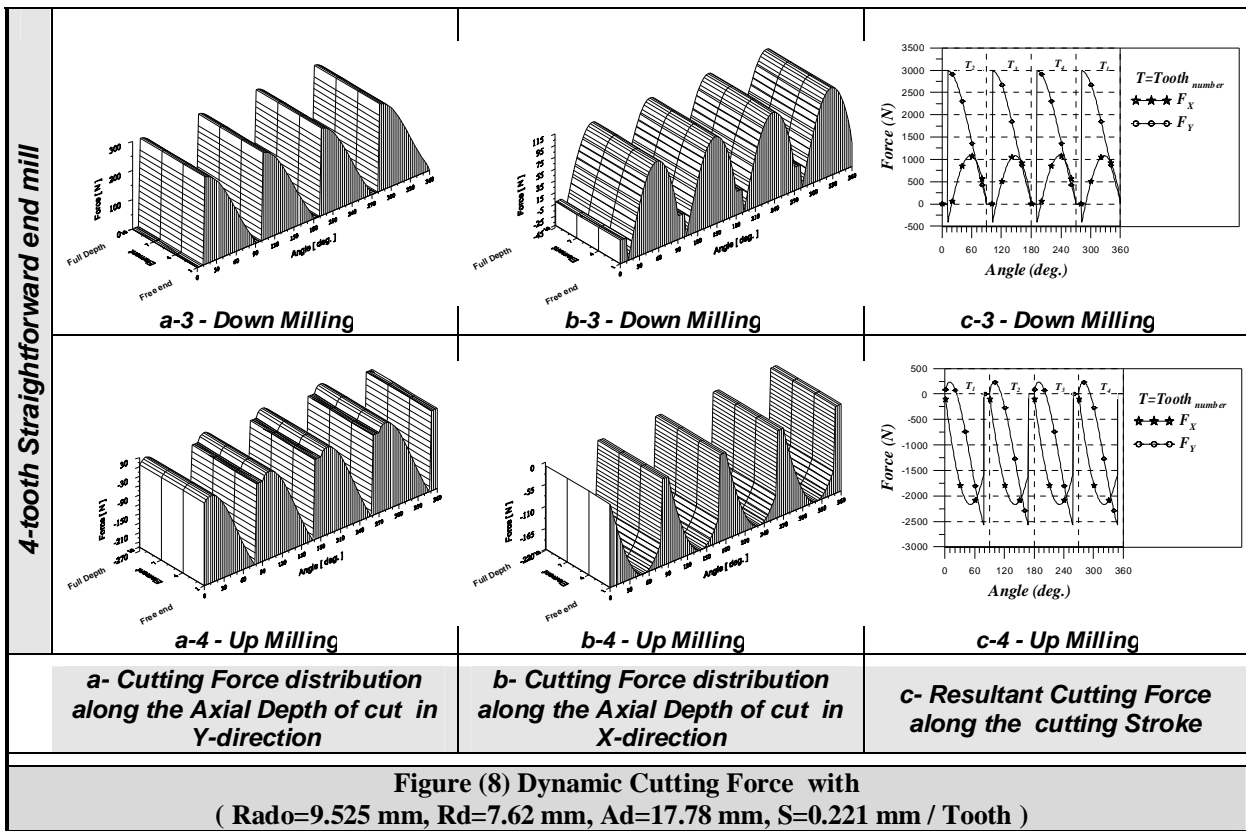
Table (1) Actual X and Y Forces and  $K_t$  and  $K_r$  values for 7075-T6 Aluminum.

| Test                         | $R_d$<br>mm | $A_d$<br>mm | S<br>mm/tooth | Measured Average Forces [9-1983 s] |              | Cutting Constants [9-1983 s]        |        | Cutting Constants [13-2008s] |          |
|------------------------------|-------------|-------------|---------------|------------------------------------|--------------|-------------------------------------|--------|------------------------------|----------|
|                              |             |             |               | $F_{xp}$ (N)                       | $F_{yp}$ (N) | $K_t$ (N/mm <sup>2</sup> )          | $K_r$  | $K_t$ (N/mm <sup>2</sup> )   | $K_r$    |
|                              |             |             |               | 1                                  | 5.334        | 33.02                               | 0.0762 | 320.27                       | 769.5386 |
| 2                            | 5.334       | 33.02       | 0.221         | 969.7076                           | 1854.8994    | 778.63428                           | 0.3764 | 783.2678                     | 0.3758   |
| 3                            | 2.286       | 33.02       | 0.0762        | 244.651                            | 355.856      | 1002.441                            | 0.5492 | 1010.4169                    | 0.5461   |
| 4                            | 2.286       | 33.02       | 0.221         | 751.7458                           | 831.8134     | 954.73                              | 0.3875 | 961.8759                     | 0.3847   |
| 5                            | 3.81        | 25.4        | 0.132         | 378.097                            | 720.6084     | 866.896                             | 0.5181 | 867.8685                     | 0.5179   |
| 6                            | 2.286       | 17.78       | 0.0762        | 142.3424                           | 195.7208     | 1057.0066                           | 0.5141 | 1053.2852                    | 0.5124   |
| 7                            | 2.286       | 17.78       | 0.221         | 355.856                            | 409.2344     | 849.937                             | 0.4087 | 846.9592                     | 0.407    |
| 8                            | 5.334       | 17.78       | 0.0762        | 151.2388                           | 507.0948     | 965.123                             | 0.6158 | 966.8001                     | 0.6163   |
| 9                            | 5.334       | 17.78       | 0.221         | 502.6466                           | 1094.2572    | 815.241                             | 0.4361 | 816.6544                     | 0.4365   |
| 10                           | 3.81        | 38.1        | 0.132         | 640.5408                           | 1152.0838    | 945.744                             | 0.4874 | 964.9846                     | 0.4814   |
| 11                           | 3.81        | 25.4        | 0.132         | 449.2682                           | 871.8472     | 1040.785                            | 0.5281 | 1041.9573                    | 0.5273   |
| 12                           | 3.81        | 25.4        | 0.132         | 435.9236                           | 742.8494     | 939.089                             | 0.4599 | 940.1003                     | 0.4591   |
| 13                           | 3.81        | 25.4        | 0.132         | 431.4754                           | 733.953      | 928.599                             | 0.4589 | 929.6022                     | 0.4582   |
| 14                           | 3.81        | 25.4        | 0.254         | 836.2616                           | 1330.0118    | 902.854                             | 0.4233 | 903.2593                     | 0.4225   |
| 15                           | 3.81        | 25.4        | 0.0226        | 80.0676                            | 222.41       | 1358.73                             | 0.7081 | 1353.8529                    | 0.7072   |
| 16                           | 6.35        | 25.4        | 0.132         | 427.0272                           | 1392.2866    | 951.97                              | 0.5127 | 950.2993                     | 0.5099   |
| 17                           | 1.27        | 25.4        | 0.132         | 244.651                            | 271.3402     | 1145.2                              | 0.5361 | 1142.5394                    | 0.5341   |
| 18                           | 3.81        | 12.7        | 0.132         | 191.2726                           | 378.097      | 891.9                               | 0.5349 | 895.5447                     | 0.5362   |
| Empirical Formula [13-2008s] |             |             |               | $K_t=563.982916*(T)^{-0.17670963}$ |              | $K_r=0.256961212*(T)^{-0.21659215}$ |        |                              |          |

Table (2) Actual and Predicted X and Y Forces for 7075-T6 Aluminum

| Test | Measured Average Forces[9-1983 s] |              | Predicted Average Forces [9-1983 s] |              | Predicted Average Forces [13-2008s] |              | Deference percentage [9-1983 s] |        | Deference percentage [13-2008s] |       |
|------|-----------------------------------|--------------|-------------------------------------|--------------|-------------------------------------|--------------|---------------------------------|--------|---------------------------------|-------|
|      | $F_{xm}$ (N)                      | $F_{ym}$ (N) | $F_{xp}$ (N)                        | $F_{yp}$ (N) | $F_{xp}$ (N)                        | $F_{yp}$ (N) | X (%)                           | Y (%)  | X (%)                           | Y (%) |
|      | 1                                 | 320.27       | 769.5386                            | 342.5114     | 934.122                             | 291.0544     | 712.4677                        | 6.9    | 21.38                           | 9.1   |
| 2    | 969.7076                          | 1854.8994    | 983.0522                            | 2001.69      | 916.0756                            | 1813.407     | 1.37                            | 7.91   | 5.53                            | 2.23  |
| 3    | 244.651                           | 355.856      | 240.2028                            | 364.7524     | 240.792                             | 348.824      | 1.81                            | 2.5    | 1.577                           | 1.976 |
| 4    | 751.7458                          | 831.8134     | 671.6782                            | 827.3652     | 735.372                             | 819.377      | 10.65                           | 0.53   | 2.178                           | 1.495 |
| 5    | 378.097                           | 720.6084     | 427.0272                            | 756.194      | 410.137                             | 784.836      | 12.94                           | 4.93   | 8.474                           | 8.91  |
| 6    | 142.3424                          | 195.7208     | 137.8942                            | 213.5136     | 134.0563                            | 181.1782     | 3.12                            | 9.09   | 5.82                            | 7.43  |
| 7    | 355.856                           | 409.2344     | 360.3042                            | 444.82       | 360.7411                            | 421.4719     | 1.25                            | 8.69   | 1.37                            | 2.99  |
| 8    | 151.2388                          | 507.0948     | 186.8244                            | 511.543      | 155.223                             | 501.501      | 23.52                           | 0.87   | 2.635                           | 1.103 |
| 9    | 502.6466                          | 1094.2572    | 529.3358                            | 1080.912     | 547.8486                            | 1044.044     | 5.3                             | 1.21   | 8.99                            | 4.58  |
| 10   | 640.5408                          | 1152.0838    | 644.989                             | 1147.635     | 629.73                              | 1128.35      | 0.69                            | 0.386  | 1.687                           | 2.06  |
| 11   | 449.2682                          | 871.8472     | 427.0272                            | 756.194      | 410.137                             | 784.836      | 4.9                             | 13.265 | 8.71                            | 9.98  |
| 12   | 435.9236                          | 742.8494     | 427.0272                            | 756.194      | 410.137                             | 784.836      | 2.04                            | 1.79   | 5.915                           | 5.652 |
| 13   | 431.4754                          | 733.953      | 427.0272                            | 756.194      | 410.137                             | 784.836      | 1.03                            | 3.03   | 4.94                            | 6.93  |
| 14   | 836.2616                          | 1330.0118    | 773.9868                            | 1192.117     | 753.1909                            | 1309.036     | 7.44                            | 10.3   | 9.93                            | 1.577 |
| 15   | 80.0676                           | 222.41       | 75.6194                             | 186.8244     | 75.25813                            | 215.208      | 5.55                            | 16     | 6                               | 3.238 |
| 16   | 427.0272                          | 1392.2866    | 453.7164                            | 1263.288     | 441.3675                            | 1367.308     | 6.25                            | 9.26   | 3.35                            | 1.794 |
| 17   | 244.651                           | 271.3402     | 222.41                              | 249.0992     | 239.28                              | 264.1388     | 9.09                            | 8.19   | 2.195                           | 2.654 |
| 18   | 191.2726                          | 378.097      | 213.5136                            | 378.097      | 193.567                             | 350.3904     | 11.62                           | 0      | 1.2                             | 7.32  |





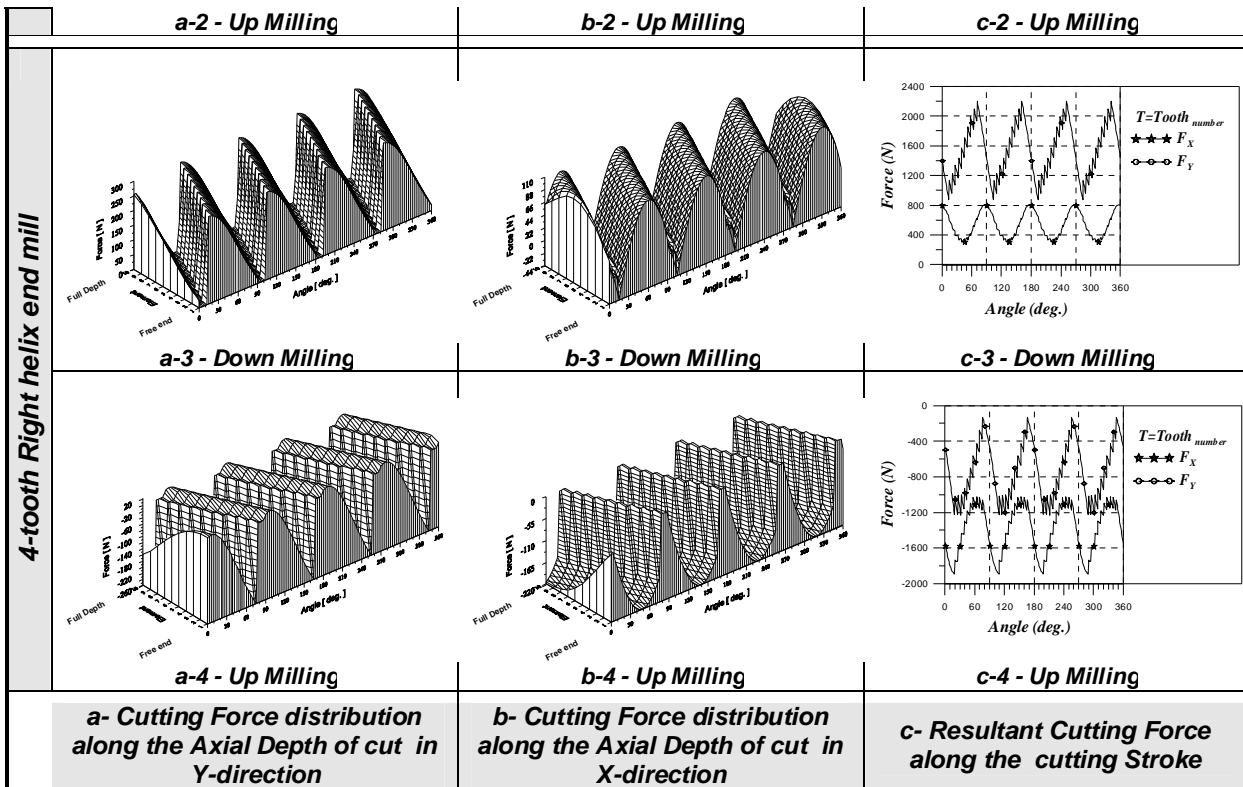
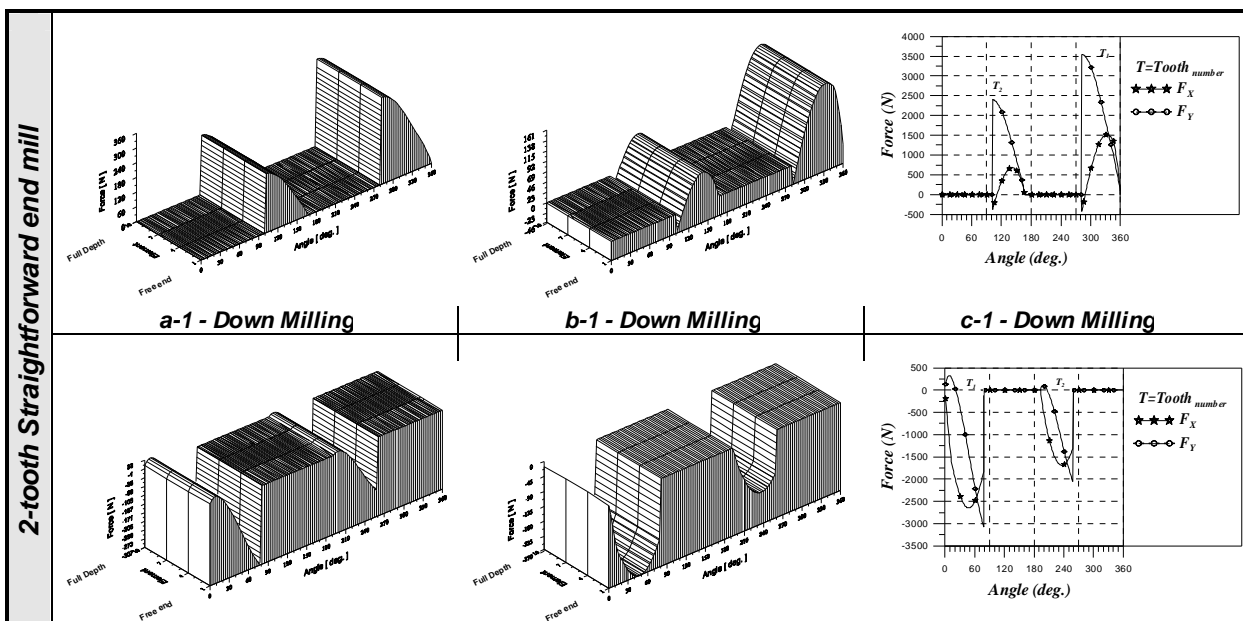


Figure (9) Dynamic Cutting Force with ( Rado=9.525 mm, Rd=7.62 mm, Ad=17.78 mm, S=0.221 mm / Tooth,  $\alpha_h=30^\circ$  )



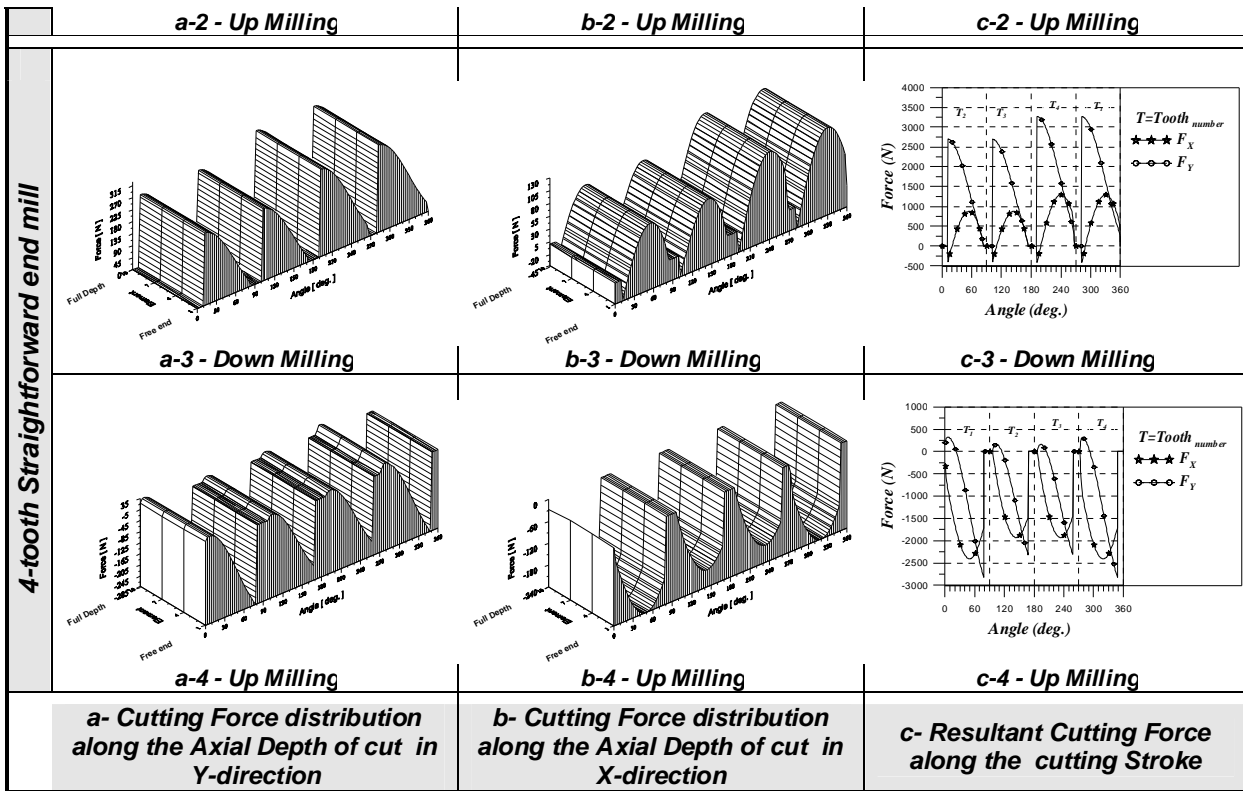
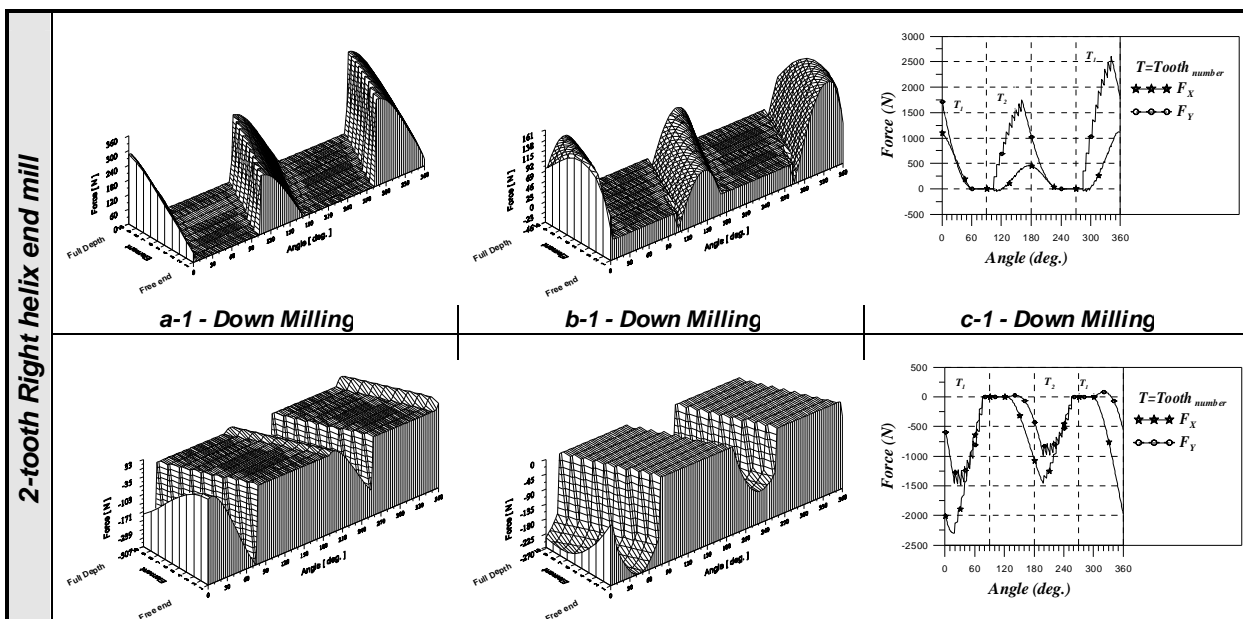


Figure (10) Dynamic Cutting Force with Run out effect & ( Rado=9.525 mm, Rd=7.62 mm, Ad=17.78 mm, S=0.221 mm / Tooth, Rn=25.4 μm, αRn=0o )



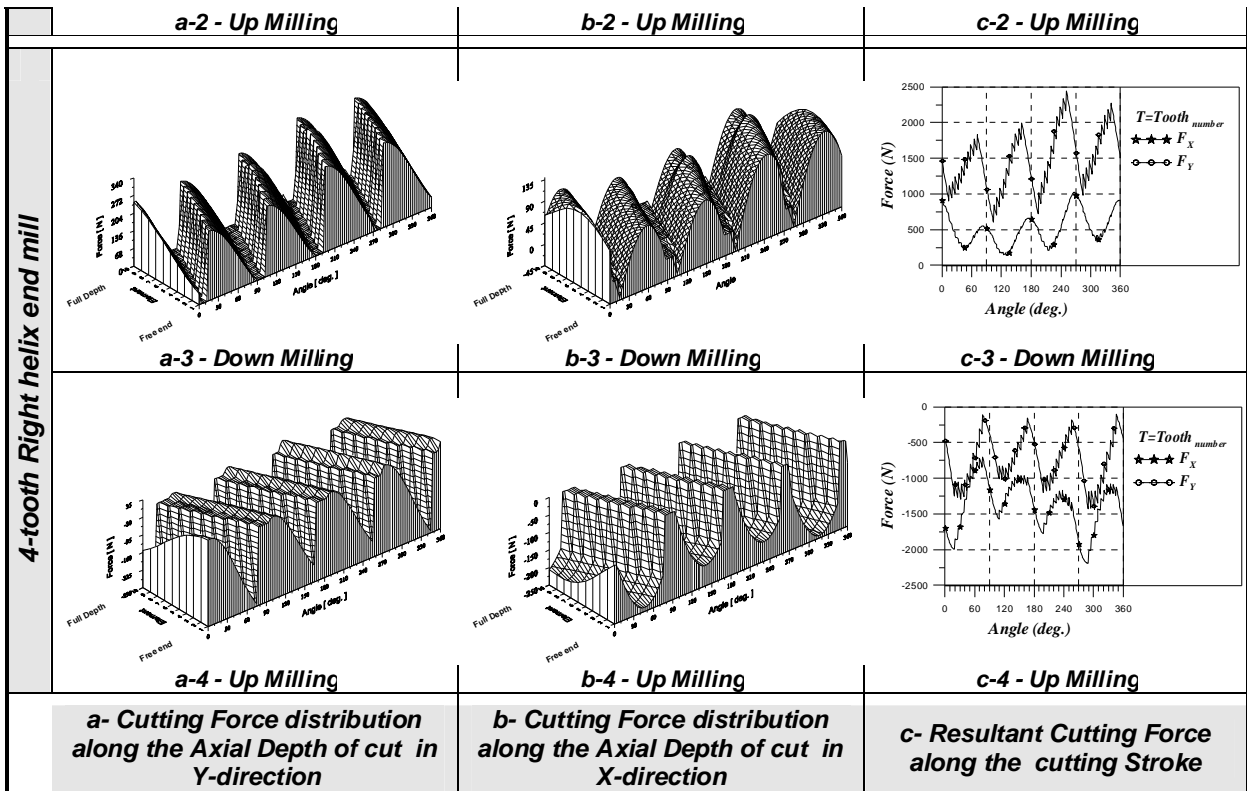
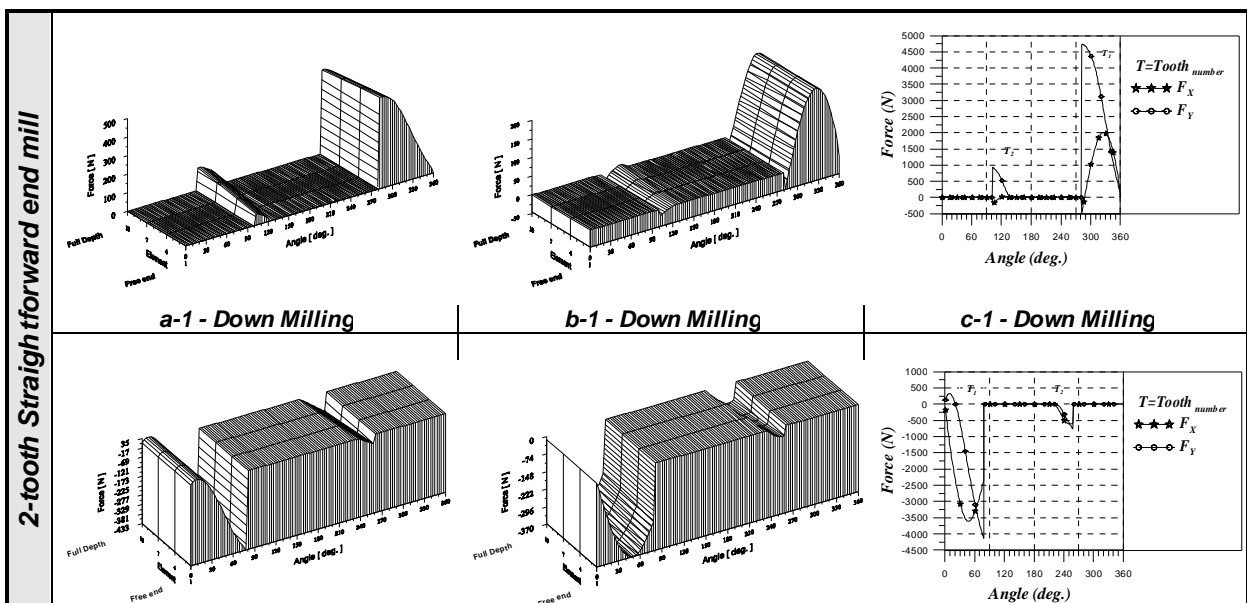
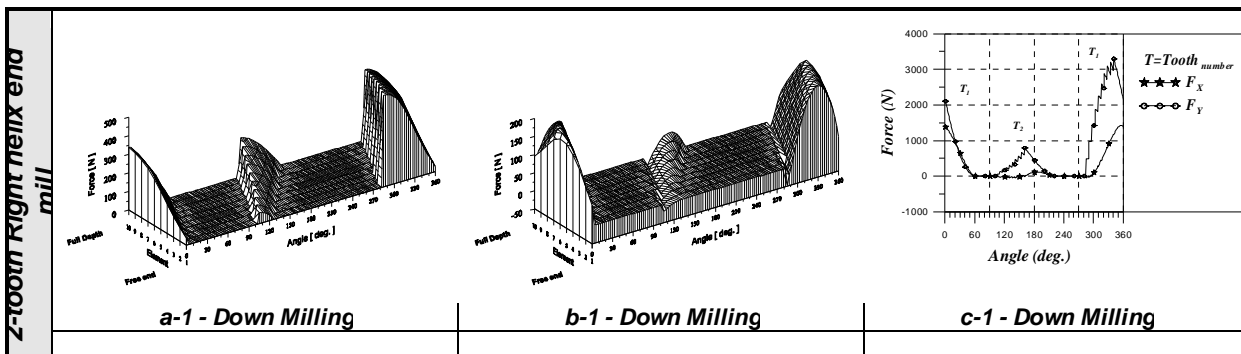
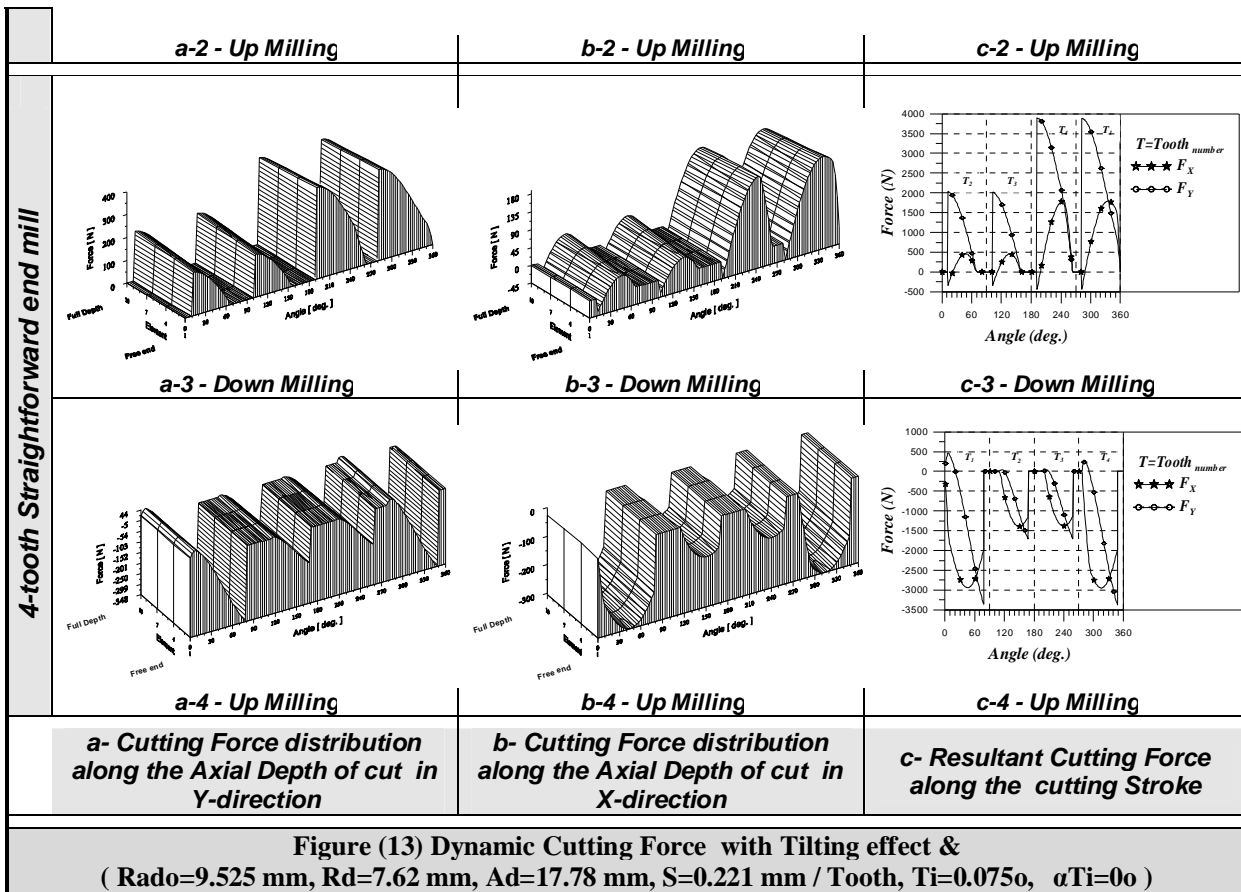
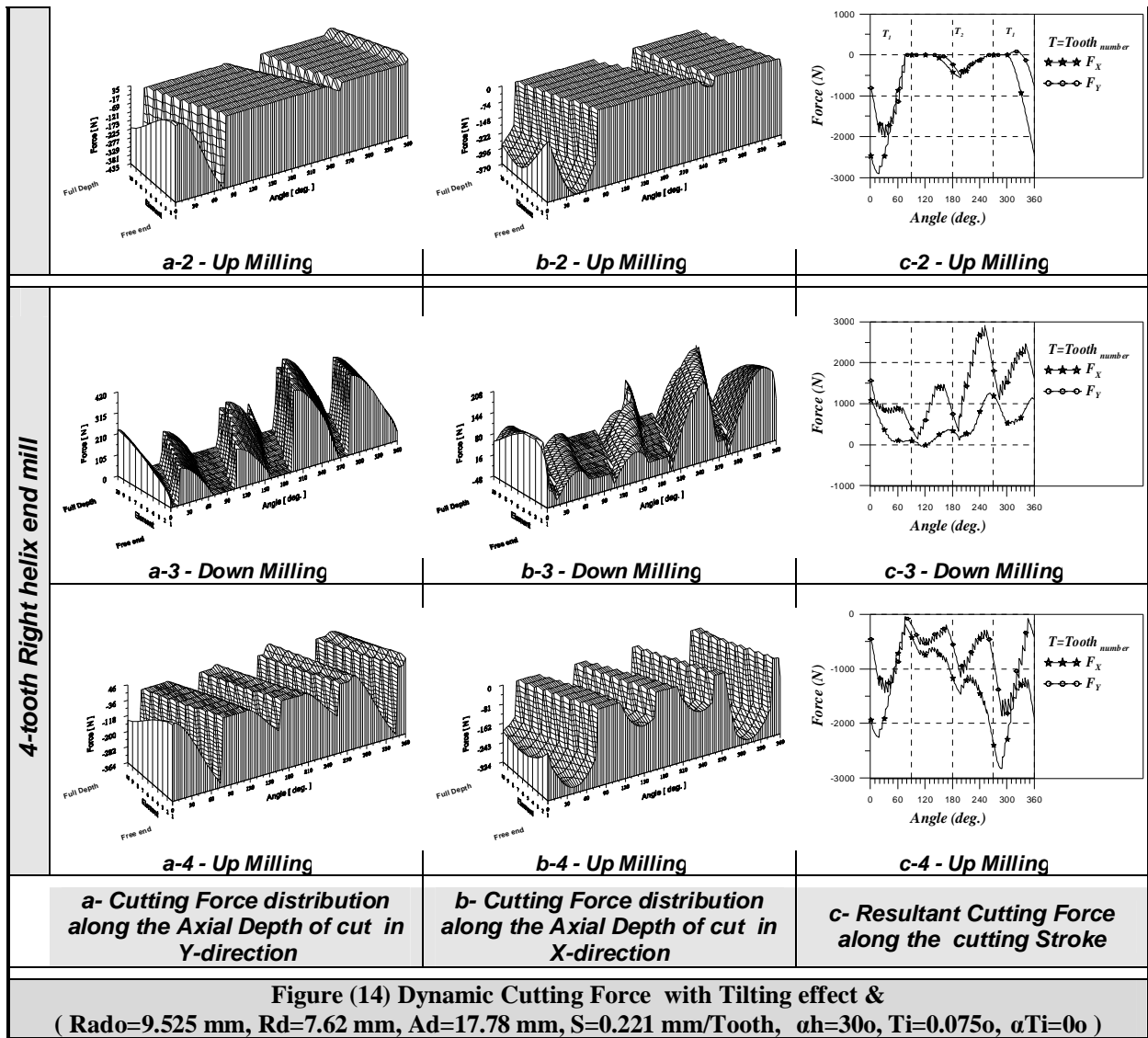
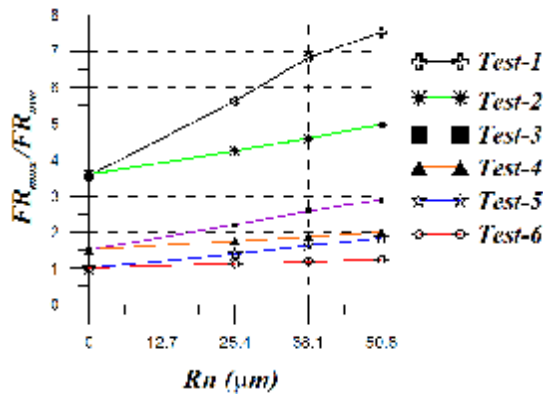


Figure (11) Dynamic Cutting Force with Run out effect & ( Rado=9.525mm, Rd=7.62mm, Ad=17.78mm, S=0.221mm/Tooth,  $\alpha_h=30^\circ$ , Rn=25.4 $\mu$ m,  $\alpha_{Rn}=0^\circ$  )



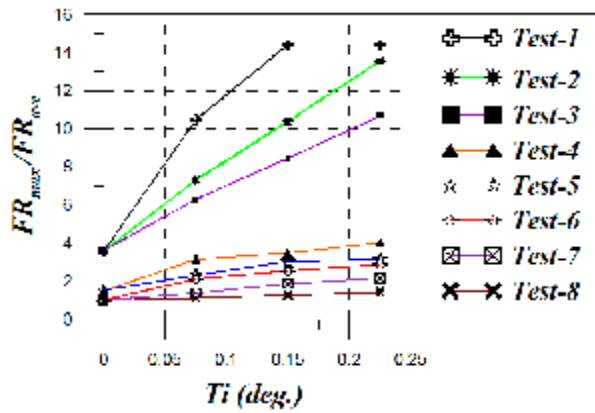






| Test | R <sub>d</sub> (mm) | A <sub>d</sub> (mm) | S (mm/Tooth) |
|------|---------------------|---------------------|--------------|
| 1    | 2.286               | 2                   | 0.0762       |
| 2    | 2.286               | 2                   | 0.221        |
| 3    | 7.62                | 14                  | 0.0762       |
| 4    | 7.62                | 14                  | 0.221        |
| 5    | 19.05               | 30                  | 0.0762       |
| 6    | 19.05               | 30                  | 0.221        |

Figure (12) Radial Run out effect on (resultant maximum per average) Force for 4-tooth Straightforward end mill with (R<sub>do</sub>=9.525 mm, α<sub>Rn</sub>=0°).



| Test | R <sub>d</sub> (mm) | A <sub>d</sub> (mm) | S (mm/Tooth) | L (mm) |
|------|---------------------|---------------------|--------------|--------|
| 1    | 2.288               | 2                   | 0.0782       | 72     |
| 2    | 2.288               | 2                   | 0.0762       | 36     |
| 3    | 2.286               | 2                   | 0.221        | 72     |
| 4    | 7.62                | 14                  | 0.0762       | 72     |
| 5    | 7.62                | 14                  | 0.221        | 72     |
| 6    | 19.05               | 30                  | 0.0762       | 72     |
| 7    | 19.05               | 30                  | 0.221        | 72     |
| 8    | 19.05               | 30                  | 0.221        | 36     |

Figure (15) Axial Tilting effect on (resultant maximum per average) Force for 4-tooth Straightforward end mill with (R<sub>do</sub>=9.525 mm, α<sub>Ti</sub>=0°).